Electron spectroscopic investigation of the semiconductor-metal transition in $La_{1-x}Sr_xMnO_3$

A. Chainani, M. Mathew, and D. D. Sarma
Solid State and Structural Chemistry Unit, Indian Institute of Science, Bangalore-560 012, India
(Received 16 November 1992; revised manuscript received 3 February 1993)

We study the electronic structure of $La_{1-x}Sr_xMnO_{3+\delta}$, $x=0$, 0.1, 0.2, 0.3, and 0.4, across the semiconductor-metal transition, using various electron spectroscopy techniques. The negligible intensity seen at E_F using ultraviolet photoemission spectroscopy and bremsstrahlung isochromat spectroscopy (BIS) indicate an unusual semiconductor-metal transition observed for $x \geq 0.2$, consistent with the resistivity data. The BIS spectra show doped hole states developing about 1.4 eV above E_F as a function of x. Auger electron spectroscopy gives an estimate of the intra-atomic Coulomb energy in the O $2p$ manifold to be about 6.8 eV. The Mn $2p$ core-level spectrum of $LaMnO_3$, analyzed in terms of a configuration-interaction calculation, gives parameter values of the charge-transfer energy $\Delta=5.0$ eV, the hybridization strength between Mn $3d$ and O $2p$ states, $t=3.8$ eV, and the on-site Coulomb energy in Mn $3d$ states $U_{dd}=4.0$ eV, suggesting a mixed character for the ground state of $LaMnO_3$.

INTRODUCTION

Transition-metal oxides exhibit a wide variety of semiconductor-metal transitions.[1,2] Among these, the series of perovskite oxides $LaMO_3$ ($M=3d$ transition metal) itself provides an interesting series of related compounds exhibiting different types of semiconductor-metal transitions. For example, while the two end members of this series, $LaTiO_3$ and $LaNiO_3$, are believed to be metallic,[3,4] the other compounds with M = V-Co are insulating.[2] Moreover, $LaCoO_3$ is believed to exhibit an insulator-metal transition between 500 and 750 K.[5] It is known that the insulating parent compounds with M = V,[6] Mn,[7] and Co (Ref. 8) can be driven into the metallic state by substituting Sr^{2+} for La^{3+}, thereby chemically doping holes into the system. In this class of composition-induced semiconductor-metal transitions, $La_{1-x}Sr_xMnO_3$ compounds exhibit the most unusual resistivity behavior.[9]

The earliest work on the electrical and magnetic properties of $La_{1-x}Sr_xMnO_3$ (Refs. 7 and 10) concluded a semiconductor-metal transition for $x \geq 0.2$. However, the resistivity (ρ) was found to exhibit a maximum at a critical temperature (T_{max}) depending on the composition of the metallic sample. The maxima in ρ vs T in the metallic samples were associated[7,10] with the ferromagnetism in these compounds. However, recently[9] it has been pointed out that these maxima cannot be attributed to the onset of ferromagnetism in the samples, since the Curie temperatures are much higher than T_{max} at all compositions. This recent study also points out several other anomalous transport properties of this series. For example, the high-temperature resistivity behavior even for the metallic samples indicates the existence of a gap comparable in magnitude to that in the parent insulator $LaMnO_3$, *suggesting that the gap in charge excitation survives on doping* and the semiconductor-metal transition is brought about on lowering the temperature. The room-temperature resistivity of the sample as a function of x changes smoothly across the critical composition x_c ($\simeq 0.2$) without any clear indication of a semiconductor-metal transition. The most unusual aspect in this system is the exceptionally high values of the resistivity for compositions that exhibit an unambiguous metallic character in ρ vs T plots. For example, ρ of the metallic $La_{0.8}Sr_{0.2}MnO_3$ is found[9,10] to be between 7 and 14 Ω cm, which is four orders of magnitude larger than that of most other metallic oxides. Even with $x=0.4$, ρ remains to be about two orders of magnitude too large. Thus it appears clear that the $La_{1-x}Sr_xMnO_3$ series exhibits an unusual semiconductor-metal transition. Besides this semiconductor-metal transition, the electronic structure of this series is also interesting in view of the potential use of these compounds as solid oxide electrodes in high-temperature fuel cells.[11,12]

To date there have been no electron spectroscopy studies of the series $La_{1-x}Sr_xMnO_3$ across the semiconductor-metal transition as a function of x, with the exception of an x-ray photoelectron spectroscopy study of $LaMnO_3$,[13] a recent study[14] analyzing the $2p$ core-level spectra of the end members $LaMnO_3$ and $SrMnO_3$, and another study[15] reporting only the oxygen $1s$ and Mn $2p$ x-ray absorption data. The values of different interaction strengths obtained in Ref. 14 suggest a charge-transfer description of the ground state in $LaMnO_3$ with $U_{dd} \simeq 2\Delta$. This is somewhat surprising since $LaCoO_3$, which belongs to the same perovskite family, has been shown[16] to have a mixed character ground state with comparable values for the intra-atomic Coulomb strength and the charge-transfer energy. Similar values have also been obtained[17] for $LiCoO_2$ where the local structure around Co^{3+} is very similar to that in $LaCoO_3$. It should be noted here that the charge-transfer energy is expected to become larger compared to the Coulomb interaction strength with decreasing atomic number in a related series of oxides, suggesting that $LaMnO_3$ should be more towards the Mott-Hubbard regime. Here we point out that the analysis of the Mn $2p$

core-level spectrum in $LaMnO_3$ presented in Ref. 14 is of very limited use due to the extensive interference from overlapping Auger signals. The x-ray absorption study of $La_{1-x}Sr_xMnO_3$,[15] on the other hand, concludes extensively mixed character for the doped hole states on the basis of a qualitative analysis. This latter study does not analyze the ground-state electronic structure of $LaMnO_3$. Most importantly, these studies do *not* relate to the unusual semiconductor-metal transition in the $La_{1-x}Sr_xMnO_3$ system. Thus we have carried out a detailed electron spectroscopic investigation of the semiconductor-metal transition in $La_{1-x}Sr_xMnO_3$ using the techniques of x-ray photoelectron (XPS), ultraviolet photoelectron (UPS), Auger electron (AES), and bremsstrahlung isochromat (BIS) spectroscopies for this series with $x=0.0$, 0.1, 0.2, 0.3, and 0.4. We determine the changes in the occupied and unoccupied density of states and show the systematic growth of doped hole states for increasing x. These experimental spectra indicate the possible reasons for the unusual semiconductor-metal transition in this series. We also obtain an estimate of the on-site Coulomb repulsion energy U_{pp} on the oxygen sites. An analysis of the Mn $2p$ core-level spectrum without any interference from an overlapping Auger spectrum gives us estimates of the charge-transfer energy (Δ) and the hybridization strength (t) between the Mn $3d$ and the symmetry adapted O $2p$ states as well as the value of U_{dd}. We find that Δ is somewhat larger than U_{dd}, though a large value of t ensures a strongly mixed character of the ground state.

EXPERIMENT

The compounds $La_{1-x}Sr_xMnO_3$, $x=0.0$–0.4, were prepared by dissolving required proportions of previously dried La_2O_3, $MnC_2O_4\cdot 2H_2O$, and $SrCO_3$ in concentrated nitric acid. The mixture was decomposed at about 400 °C and subsequently heated at 800 °C for two days. After this the mixture was ground, pelletized, and heated at 800 °C for three days; this cycle was repeated a minimum of four times and the samples were finally quenched in air. A single phase compound was obtained as determined by powder x-ray diffractometry in every case. The x-ray powder diffraction data confirmed[2,18] that the structure is an orthorhombic perovskite which changes to a rhombohedral symmetry for $x \geq 0.2$.

It is known[7] that these compounds form with excess oxygen, i.e., $La_{1-x}Sr_xMnO_{3+\delta}$. It is to be noted that the presence of excess oxygen introduces doped hole states making it necessary to estimate the value of δ. Thus the compounds were characterized for oxygen stoichiometry (or Mn^{4+} concentration) by potentiometric titrations. The compounds were dissolved in $8N$ HCl in the presence of excess ferrous ammonium sulphate (FAS) so as to reduce all the nominal Mn^{3+}/Mn^{4+} to Mn^{2+}. The remaining FAS was accurately titrated using $K_2Cr_2O_7$ to determine the oxygen content. The compositions obtained were as follows: $LaMnO_{3.13}$, $La_{0.9}Sr_{0.1}MnO_{3.12}$, $La_{0.8}Sr_{0.2}MnO_{3.10}$, $La_{0.7}Sr_{0.3}MnO_{3.06}$, and $La_{0.6}Sr_{0.4}MnO_{3.04}$. Hence we measure a systematic increase in Mn^{4+} content for increasing Sr content over and above the 26% Mn^{4+} measured for $x=0$. Thus we obtain 34% Mn^{4+} content for the $x=0.1$ sample due to a small compensating decrease in oxygen content. Similarly, we measure a total Mn^{4+} content of 40% for $x=0.2$, 42% for $x=0.3$, and 48% for $x=0.4$, respectively, in good agreement with earlier data.[10] The XPS, UPS, AES, and BIS measurements were carried out in a combined XPS-UPS-BIS electron spectrometer of VSW Scientific Instruments Ltd., Manchester. All experiments were performed on well-sintered pellets at a vacuum of about 7×10^{-10} torr. The XP spectra were recorded using a Mg $K\alpha$ source with a total resolution of about 0.8 eV, except for the Mn $2p$ core-level spectra which were recorded using an Al $K\alpha$ source with a resolution of about 1.0 eV. This was necessitated by the fact that the Mn LMV and LNN Auger signals overlap the Mn $2p_{1/2}$ and $2p_{3/2}$ features when Mg $K\alpha$ radiation is used. The UP spectra were recorded using He I radiation from a discharge lamp with a total resolution of 140 meV. The BIS data were acquired using an incident electron-beam current of 100 μA at a fixed photon energy of 1486.6 eV. The resolution in this case was about 0.8 eV. The Fermi level was determined from the spectra of the copper stub on which the samples were mounted. No surface charging was observed for the semiconducting samples. The experiments were performed at the liquid-nitrogen temperature to avoid surface degradation. The cleanliness of the sample surface was ensured by *in situ* scraping of the surface with an alumina file. The C $1s$ signal due to carbonate impurity was negligible in all the samples. A check for possible degradation of the sample surface during BIS measurements was done by recording the O $1s$ signal after the BIS measurements and it showed no change. We also point out that the existence of the semiconductor-metal transition was established for the samples from resistivity measurements that were then studied using the electron spectroscopies. The resistivity data for the samples are very similar to that reported earlier.[7,9]

RESULTS AND DISCUSSION

In Fig. 1 we show the x-ray photoelectron spectra in the valence-band regions of $La_{1-x}Sr_xMnO_{3+\delta}$ for all values of x. Undoped $LaMnO_{3+\delta}$ ($\delta=0.13$) exhibits its most prominent peak about 5.8 eV below E_F. A prominent shoulder at about 3.4-eV binding energy can also be seen clearly in the spectrum. There is a low-intensity shoulder close to E_F in this spectrum, the tail of which comes close to E_F. The position of E_F with respect to this feature suggests that the Fermi level in this material is close to the top of the valence band, presumably due to the existence of excess oxygen. In this context it should be noticed that the presence of excess oxygen ($\delta>0.0$) effectively dopes holes near the top of the valence band. However, we find that there is hardly any intensity in this spectrum at the Fermi energy, consistent with the fact that $LaMnO_3$ is an insulator with a resistivity band gap[9] of about 0.24 eV.

On substituting La by Sr in $La_{1-x}Sr_xMnO_{3+\delta}$, several small changes are seen in the spectra of the valence-band

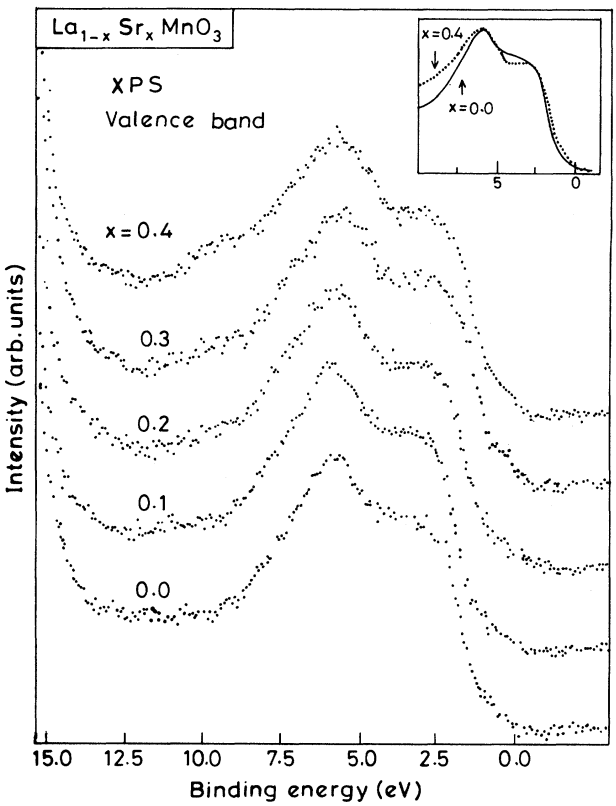

FIG. 1. The XPS valence-band spectra of $La_{1-x}Sr_3MnO_3$, $x=0.0$–0.4, using Mg $K\alpha$ radiation. The inset shows the $LaMnO_3$ spectrum in comparison with $La_{0.6}Sr_{0.4}MnO_3$.

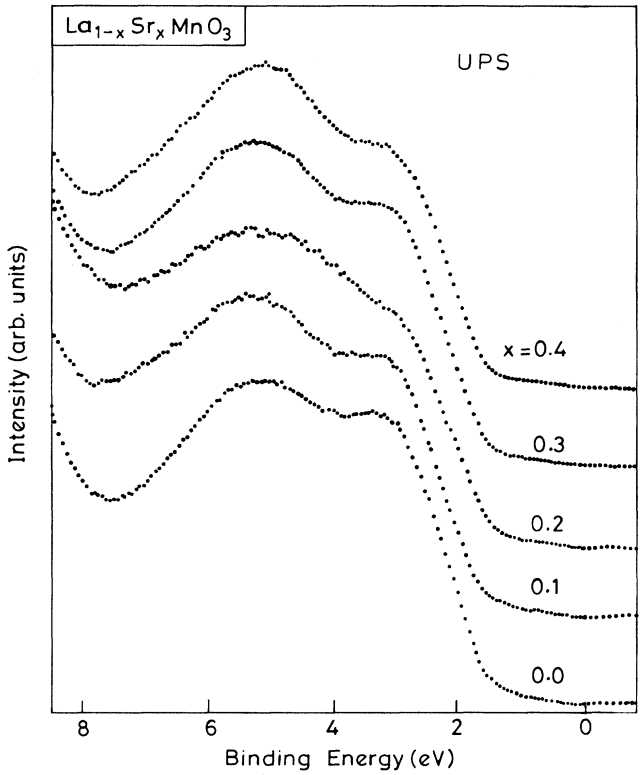

FIG. 2. The He I UPS spectra of $La_{1-x}Sr_3MnO_3$, $x=0.0$–0.4. Note the negligible intensity at E_F even for the metallic compositions, $x \geq 0.2$.

regions (Fig. 1). A feature is seen to grow in intensity with increasing Sr content at about 9.5-eV binding energy. This feature is due to the $\alpha_{3,4}$ satellite of Sr $4p$ signal appearing at 18.6-eV binding energy. Besides this artifact we find subtle but systematic changes in the spectral shape within about 5 eV of E_F, while the main peak at about 5.8 eV remains relatively unaltered in this family of compounds. Thus we compare the spectral features arising from semiconducting $LaMnO_3$ and metallic $La_{0.6}Sr_{0.4}MnO_3$ in the inset of Fig. 1. From this comparison it is clear that the spectral intensity decreases near about 4.0-eV binding energy, while it increases slightly between E_F and about 2-eV binding energy on hole doping due to the substitution of Sr^{2+} for La^{3+}. This redistribution of spectral weight is attributed to changes in the character of the ground-state wave function on hole doping. This point is further supported by the analysis of the Mn $2p$ core-level spectra, as discussed later in the text. It is interesting to note here that there is hardly any increase in the spectral intensity at E_F in the Sr substituted samples compared to that in $LaMnO_3$. This is in conformity with the high-temperature resistivity data suggesting that the gap in the charge excitation spectrum survives even in the presence of chemical doping of holes in these oxides.

We show the ultraviolet photoemission spectra from these compounds using He I radiation in Fig. 2. For $LaMnO_3$, the most intense peak in this case appears at 5.3 eV and a second feature of nearly equal intensity at about 3.4 eV. Besides these two prominent signals, we find evidence for the existence of a low-intensity signal within the first 1.0-eV binding energy tailing towards E_F. However, the spectral intensity is negligible at E_F for $LaMnO_3$. These three spectral features in the UP spectra correspond quite well with those obtained from x-ray photoemission experiments shown in Fig. 1. It is to be noted here that the Mn $3d$ cross section for photoionization dominates the spectral shape at Mg $K\alpha$ energy, while the states arising from oxygen $2p$ become more important with He I radiation.[19] Thus the observation that the two prominent peaks and the weak signal near E_F in UP spectra have similar intensity as in the XP spectra (see Figs. 1 and 2) suggests that these spectral signatures arise from extensively hybridized Mn $3d$–O $2p$ states. On doping $LaMnO_3$ with holes by the substitution of La^{3+} with Sr^{2+}, we find that the spectral feature at about 3.4-eV binding energy systematically decreases in intensity, consistent with the observation of a similar decrease in intensity in the XP spectra (Fig. 1). Here it is important to notice the absence of any spectral intensity at E_F in the UP spectra of $La_{1-x}Sr_xMnO_{3+\delta}$ for all x values. As pointed out earlier, the XP spectra in Fig. 1 are also consistent with the above observation; however, the UP spectra establish the fact more convincingly due to the better resolution in this technique. It is improbable that the states at E_F have such a low photoionization cross section both at He I and Mg $K\alpha$ photon energies, that it

is entirely missed in this technique. Thus it appears that $La_{1-x}Sr_xMnO_3$ with $x=0.0-0.4$ exhibits a gap (or a pseudogap with very low density of states) of comparable magnitude in the single-particle density of states at E_F for all the compositions. This is consistent with the high-temperature resistivity data discussed earlier, which indicated that a conductivity gap of about 0.2 eV exists for all compositions at $T>300$ K. However, these spectra were recorded with a sample temperature of about 80 K, where all the samples with $x \geq 0.2$ are metallic and do not exhibit the activated behavior in the resistivity data. We find that the room-temperature spectra of these compounds are identical to those of Fig. 2 recorded at 80 K. Thus it appears that the underlying gap at high temperatures for all x does not collapse with the lowering of temperature. In view of this, the low-temperature metallic behavior for $x \geq 0.2$ is indeed surprising. The metallic property in such a situation can come about in two different ways. One is the possibility that the small gap at high temperature is closed by a very low density of states at lower temperature due to the tailing of the states near E_F; this density of states will have to be low enough to be undetectable by the photoemission experiments reported here. The other possibility is that the single-particle density of states continues to have the gap even at lower temperatures, consistent with the results of Fig. 2, while multielectron processes, which are expected to be of increasing importance for conductivity with decreasing temperature,[20] introduce the metallic behavior observed for $x \geq 0.2$ in $La_{1-x}Sr_xMnO_3$. Both these possibilities are consistent with the unusually high-resistivity values of the metallic samples.

The BI spectra of $La_{1-x}Sr_xMnO_3$ exhibit an intense peak at about 8.7 eV above E_F attributed primarily to the La $4f$ states and a weaker intensity feature nearer to E_F due to transitions into the upper Hubbard band formed by hybridizing the Mn $3d$ states with oxygen $2p$ states constituting the conduction band. For the sake of clarity we show only the conduction-band region for each of the compounds (Fig. 3). In $LaMnO_3$ this feature peaks at about 2.4 eV above E_F with a substantial tailing towards E_F. The nearly negligible intensity at E_F arises from resolution and lifetime broadening. A simple estimate for the upper limit of the band gap obtained from this spectrum is about 0.6 eV, as shown in Fig. 3. This value is in rough agreement with the band gap obtained from the resistivity data. However, if we take the midpoint of the rising part of this peak near E_F as an indication of the band gap, we obtain a somewhat larger value (1.3 eV) for the band gap. It is indeed possible that the band gap in stoichiometric $LaMnO_3$ will be closer to 1.3 eV and the excess oxygen in $LaMnO_{3.13}$ dopes hole states below the conduction band leading to a decrease of the band gap to 0.24 eV as observed in resistivity data. On doping the compounds with holes, we find that the peak position (about 2.4 eV above E_F) for the upper Hubbard band does not shift within the experimental uncertainty, while the spectral intensity between this peak position and E_F increases systematically with increasing x leading to a more pronounced broadening towards E_F. In order to observe the changes in the spectral shape, we have obtained the difference spectra between $La_{1-x}Sr_xMnO_3$ ($x>0$) and $LaMnO_3$; these are shown in Fig. 4. From this figure we find that new states emerge with a peak position about 1.4 eV above E_F on doping the parent compound with Sr. These doped states thus peak closer to E_F compared to the peak position (about 2.4 eV above E_F) of the upper Hubbard band. These new states for $x>0$ are attributed to the doped hole states due to the formation of formal Mn^{4+} on hole doping. We also find that the spectral intensity of these doped states progressively increases with increasing x, while the peak position remains unaltered at about 1.4 eV within the experimental uncertainty (see Fig. 4). Moreover, it is seen that the intensity at E_F from these doped states is rather small, virtually indistinguishable from the contribution arising from the resolution and lifetime broadening of the states above E_F in all cases. This observation is in sharp contrast to other oxide systems such as $La_{2-x}Sr_xCuO_4$,[21] $YBa_2Cu_3O_{6.5+\delta}$,[22] and $La_{1-x}Sr_xCoO_3$ (Ref. 16) exhibiting insulator-to-metal transitions on hole doping. In these series, the doped hole states probed by BIS or x-ray absorption spectroscopy are found to generate empty states which overlap the Fermi energy with considerable density of states for the metallic compositions providing unambiguous spectral signature of the electronic transi-

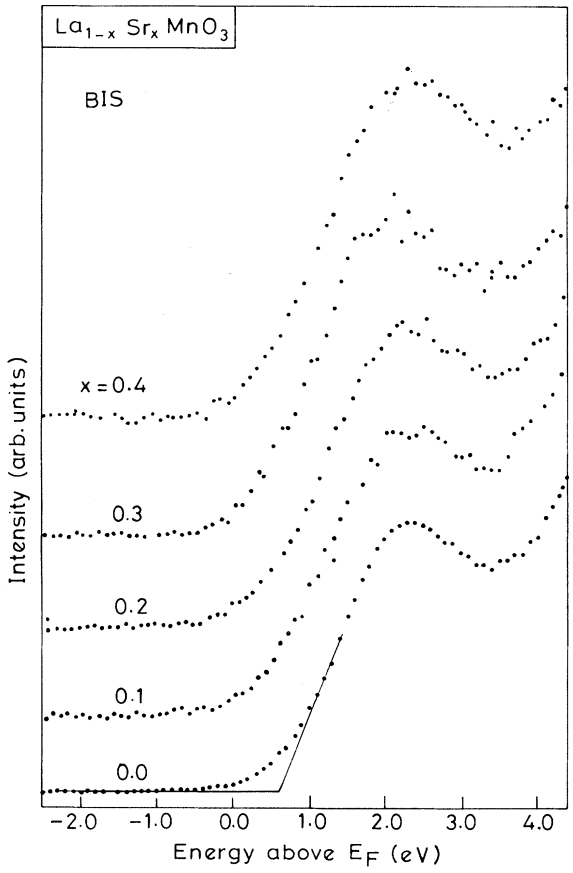

FIG. 3. The BIS near the E_F region on an expanded scale.

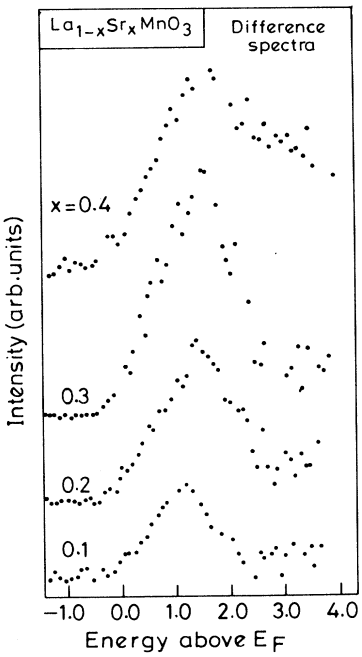

FIG. 4. The difference between the spectra of $La_{1-x}Sr_xMnO_3$, $x=0.1-0.4$, and that of $LaMnO_3$, showing the systematic increase in doped hole states centered at about 1.4 eV above E_F.

tion. In contrast, we find here a persistent absence (or near absence) of any density of states at E_F even for the metallic compositions ($x \geq 0.2$). It should be noted that the observed resistivity gap of about 0.2 eV for $La_{0.9}Sr_{0.1}MnO_3$ is in agreement with the position and line shape of the difference spectrum for this composition shown in Fig. 4. It is indeed interesting that the line shape of this difference spectrum is almost identical to those obtained for $x \geq 0.2$, which represent metallic compositions. The BIS results along with the results from the occupied part of the density of states obtained with XPS and UPS in this series appear to suggest either the existence of a gap or the presence of a very low density of states at E_F in the one-particle density of states of these oxides at all compositions. This unusual behavior of the density of states near E_F in these systems is then responsible for the unusual resistivity data of these samples.[9]

Having obtained a microscopic description for the unusual behavior of the density of states near E_F, responsible for the transport properties, we now turn to provide quantitative estimates for the various interaction strengths that govern the gross electronic structure of the parent insulating compound. Unfortunately, it was not possible for us to extract the intra-atomic Coulomb interaction strength within the Mn $3d$ manifold, U_{dd}, directly from the Mn L_{23}-$M_{45}M_{45}$ Auger spectra, due to an extensive overlap of this signal with that arising from La M_{45}-$N_{45}N_{45}$ Auger transitions. In order to extract the Coulomb correlation strength within the oxygen $2p$ states, we have recorded the oxygen K-$L_{23}L_{23}$ Auger spectra from these compounds. There is no significant change in the spectral features between the compounds with different x values, indicating very similar U_{pp} for all the compounds; this suggests that the intra-atomic Coulomb repulsion is not significantly modified by metallic screening in these oxides. Comparing these Auger spectra with the self-convoluted density of valence-band states as obtained from the x-ray photoelectron spectra (Fig. 1), we estimate a U_{pp} value of about 6.8 eV; this value is similar to the one obtained for U_{pp} in $La_{1-x}Sr_xCoO_3$ series.[16] However, if we associate the peak at about 5.5 eV in XP and UP valence-band spectra of $LaMnO_3$ (Figs. 1 and 2) with O $2p$ states, the estimate of U_{pp} turns out to be about 5.0 eV. Thus it appears that U_{pp} is, in any case, quite large in these oxides.

We find that the Mn $2p$ core-level spectra for different x values appear to be very similar, with the peak position remaining identical in all cases. A probable reason for the absence of pronounced changes in the Mn $2p$ spectra for different x values may be that the Mn $2p$ core-level spectra from $LaMnO_3$ and $SrMnO_3$ are rather similar, as can be observed in the reported data in Ref. 14. However, we find that there is a small increase in the full width at half maxima (FWHM) with increasing x; thus for the $2p_{3/2}$ core-level spectra, the FWHM is 4.1 eV for $LaMnO_3$, 4.3 eV for $La_{0.9}Sr_{0.1}MnO_3$, and about 4.5 eV for $x \geq 0.2$. In all these spectra, the $2p_{3/2}$ core-level binding energy appears at about 642.1 eV and the $2p_{1/2}$ core levels are at about 653.6 eV. Besides these main features, a broad, weak-intensity satellite is also observed at about 665.3-eV binding energy. This satellite can be ascribed to the poorly screened final state[23] associated with the $2p_{1/2}$ core-level ionization, while the main peak corresponds to the well-screened final state. Noting that the energy difference between the satellite and the $2p_{1/2}$ main peak signal is 11.7 eV, it is understood that the satellite peak associated with the $2p_{3/2}$ photoionization will overlap the $2p_{1/2}$ main peak, the spin-orbit splitting of the Mn $2p$ level being about 11.5 eV. It is possible to extract the various parameter strengths, namely the Mn $3d-O$ $2p$ hybridization strength, the bare charge-transfer energy Δ between these two levels, and the intra-atomic Coulomb interaction strength U_{dd} within the Mn $3d$ level, by analyzing the Mn $2p$ core-level spectra in terms of configuration interaction within a cluster model.[14,16,24–26] The calculational details are the same as in the case of $LaCoO_3$.[16] We define the charge-transfer energy Δ as the energy difference between $|t^3_{2g\uparrow}e^1_{g\uparrow}\rangle$ and $|t^3_{2g\uparrow}e^2_{g\uparrow}\underline{L}^1_{\sigma\downarrow}\rangle$ configurations with $\underline{L}^1_\sigma$ representing a hole in the ligand level L_σ. The energy difference between the configurations $|t^3_{2g\uparrow}t^1_{2g\downarrow}e^1_{g\uparrow}e^0_{g\downarrow}\underline{L}^1_{\pi\uparrow}\rangle$ and $|t^3_{2g\uparrow}t^0_{2g\downarrow}e^1_{g\uparrow}e^1_{g\downarrow}\underline{L}^1_{\sigma\uparrow}\rangle$ depends on the crystal field splitting as well as the oxygen-oxygen interaction strengths and has been fixed at 1.0 eV, and the exchange interaction strength is assumed to be 0.5 eV. We further constrained t_π to be half of t_σ and U_{dc} to be about 1.1 times U_{dd}.[14,16,25,26] The best fit to the experimental spectrum of $LaMnO_3$ is obtained for $\Delta=5.0$ eV, $t_\sigma=3.8$ eV, and $U_{dd}=4.0$ eV (Fig. 5). Among these three parameters, the calculated spectral shape is sensitively dependent on the value of t_σ. The ground state of $LaMnO_3$ with the above parameters turns out to have about 50% d^4, 41% $d^5\underline{L}^1$,

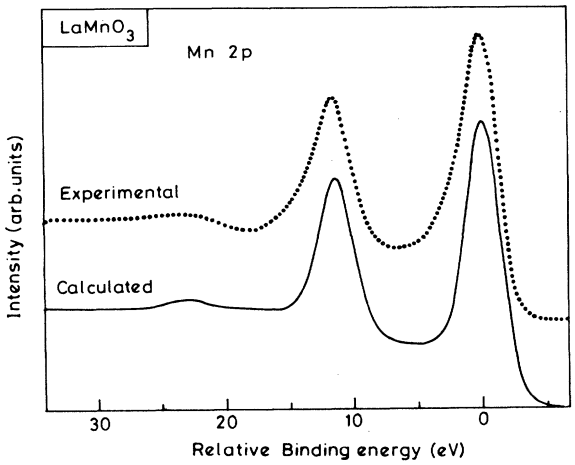

FIG. 5. The results of the configuration-interaction calculation (continuous line) compared with the experimental (dots) Mn $2p$ core-level spectrum.

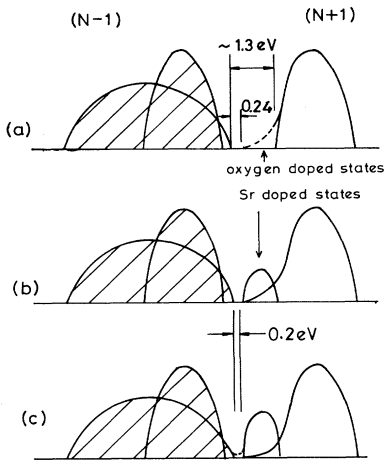

FIG. 6. Schematic description of the electronic structure and the semiconductor-metal transition in $La_{1-x}SrMnO_{3+\delta}$ in terms of the electron-removal (shaded parts) and electron-addition (unshaded parts) spectra; for (a) $LaMnO_{3+\delta}$ with $\delta > 0$, (b) $La_{1-x}Sr_xMnO_{3+\delta}$ with $0.2 > x > 0$, and (c) $La_{1-x}Sr_xMnO_{3+\delta}$ with $x \geq 0.2$.

and 9% $d^6\underline{L}^2$ states. Thus, in spite of a large value of Δ, the ground state is found to be a strongly mixed configuration due to the presence of a sizable hybridization strength t_σ. While the values of Δ and t_σ obtained here are similar to the ones obtained in Ref. 14, the present estimate of U_{dd} is somewhat smaller. While the previous estimate would have placed $LaMnO_3$ in the charge-transfer insulator regime, the present evaluation favors a more Mott-Hubbard insulatorlike description, though the large value of t ensures a very mixed character of the ground states. With the same parameter values, it is easy to see that in presence of a doped hole the energy difference between formal Mn^{4+} $3d^3$ ionic state and the corresponding charge transferred state $3d^4\underline{L}_\sigma^1$ is about 1.5 eV with the $3d^3$ state having lower energy. However, this energy difference is small compared to the hybridization strength t_σ, thereby indicating that the doped hole states will have strongly mixed Mn $3d$ and O $2p$ character, in accordance with the suggestion made in Ref. 15.

Putting together all the results with supporting evidence from the resistivity data discussed in the Introduction, we suggest the schematic diagram shown in Fig. 6 for the electronic structure of the $La_{1-x}Sr_xMnO_3$ system. In $LaMnO_3$ [Fig. 6(a)], the lower Hubbard band overlaps the oxygen $2p$ derived band leading to strong mixing of the Mn $3d$ and O $2p$ derived states, as evidenced by a comparison of XPS and UPS valence-band spectra (Figs. 1 and 2) as well as by the analysis of the Mn $2p$ spectrum (Fig. 5). The band gap in stoichiometric $LaMnO_3$ would be about 1.3 eV as inferred from the BI spectrum. However, the presence of excess oxygen leads to the formation of hole states [shown as a dashed line in Fig. 6(a)] leading to a small band gap in $LaMnO_{3.13}$, as discussed in connection with the BI spectra. Small doping of Sr ($x < 0.2$) leads to the formation of hole states at approximately the same energy where the excess oxygen-induced states are present [Fig. 6(b)]. This leads to only a marginal decrease of the band gap. With increased Sr doping ($x \geq 0.2$), the intensity of these doped hole states increases with a simultaneous decrease of the hole states induced by excess oxygen [Fig. 6(c)], as the oxygen content reduces progressively with increasing x. The gross features of the gap seen with $x = 0.1$ [Fig. 6(b)] persists even at the higher x values [Fig. 6(c)], with the possible existence of very low density of states [shown as a dashed line in Fig. 6(c)] giving rise to the metallic behavior. Alternately, the low density of states may arise from multielectron processes, while the single-particle density of states continue to have a gap.

In conclusion, we have shown that the changes in the density of states on hole doping in $La_{1-x}Sr_xMnO_3$ near E_F are very unusual and different compared to other hole doped systems like $La_{2-x}Sr_xCuO_4$,[21] $YBa_2Cu_3O_{6.5+\delta}$,[22] and $La_{1-x}Sr_xCoO_3$.[16] In $La_{1-x}Sr_xMnO_3$ with $x \geq 0.1$, we find that the doped hole states contribute intensity at about 1.4 eV above E_F with almost no intensity at E_F beyond the resolution broadening of the spectra; the spectral features are consistent with the band gap of about 0.2 eV observed near room temperature in the resistivity data of these samples. This is further supported by the absence of any intensity at or near E_F in UP spectra. These unusual behavior of the doped hole states parallels the very anomalous resistivity data of these samples. The analysis of Mn $2p$ core-level spectra suggests a very mixed character of the ground state for the parent insulating compound $LaMnO_3$ with Δ, U_{dd}, and t_σ being of comparable magnitude.

ACKNOWLEDGMENTS

We thank Professor C. N. R. Rao and Professor C. M. Varma for discussions. Financial support from the Department of Science and Technology and the Department of Atomic Energy, Government of India, is acknowledged. A.C. and M.M. thank the Council of Scientific and Industrial Research for financial support.

[1]N. Tsuda, K. Nasu, A. Yanase, and K. Siratori, *Electronic Conduction in Oxides* (Springer-Verlap, Berlin, 1990); C. N. R. Rao and J. Gopalakrishnan, *New Directions in Solid State Chemistry* (Cambridge University Press, Cambridge, England, 1986).

[2]J. B. Goodenough, *Progress in Solid State Chemistry Vol. 5*, edited by H. Reiss (Pergamon, London, 1971), p. 145.

[3]D. A. Crandles, T. Timusk, and J. E. Greedan, Phys. Rev. B **44**, 13 250 (1991); F. Lichtenberg, D. Widmer, J. G. Bednorz, T. Williams, and A. Reller, Z. Phys. B **82**, 211 (1991).

[4]K. Sreedhar, J. M. Honig, M. Darmin, M. McElfresh, P. M. Shand, J. Xu, B. C. Crooker, and J. Spalek, Phys. Rev. B **46**, 6382 (1992), and references therein.

[5]G. Thornton, B. C. Tofield, and D. E. Williams, Solid State Commun. **44**, 1213 (1982).

[6]P. Dougier and P. Hagenmuller, J. Solid State Chem. **15**, 158 (1975).

[7]J. H. Van Santen and G. H. Jonker, Physica **16**, 599 (1950).

[8]G. H. Jonker and J. H. Van Santen, Physica **19**, 120 (1953).

[9]A. Chainani, M. Mathew, D. D. Sarma, I. Das, and E. V. Sampathkumaran, Proceedings of the Conference on Strongly Correlated Electron Systems, Tokyo, 1992 [Physica B (to be published)].

[10]G. H. Jonker and J. H. Van Santen, Physica **16**, 337 (1950).

[11]T. Takahashi and H. Iwahara (unpublished).

[12]A. Hammouche, E. Siebert, and A. Hammou, Mater. Res. Bull. **24**, 369 (1989).

[13]D. J. Lam, B. W. Veal, and D. E. Ellis, Phys. Rev. B **22**, 5730 (1980).

[14]A. E. Bocquet, T. Mizokawa, T. Saitoh, H. Namatame, and A. Fujimori, Phys. Rev. B **46**, 3771 (1992).

[15]M. Abbate, F. M. F. de Groot, J. C. Fuggle, A. Fujimori, O. Strebel, F. Lopez, M. Domke, G. Kaindl, G. A. Sawatzky, M. Takano, Y. Takeda, H. Eisaki, and S. Uchida, Phys. Rev. B **46**, 4511 (1992).

[16]A. Chainani, M. Mathew, and D. D. Sarma, Phys. Rev. B **46**, 9976 (1992).

[17]J. Van Elp, J. L. Wieland, H. Eskes, P. Kuiper, G. A. Sawatzky, F. M. F. de Groot, and T. S. Turner, Phys. Rev. B **44**, 6090 (1991).

[18]A. Wold and R. J. Arnott, J. Phys. Chem. Solids **9**, 176 (1959); B. C. Tofield and W. R. Scott, J. Solid State Chem. **10**, 183 (1974).

[19]J. J. Yeh and I. Lindau, At. Data Nucl. Data Tables **32**, 1 (1985).

[20]M. Pollak and M. L. Knotek, J. Non-Cryst. Solids **32**, 141 (1979).

[21]C. T. Chen *et al.*, Phys. Rev. Lett. **66**, 104 (1991): J. A. Yarmoff *et al.*, Phys. Rev. B **36**, 3967 (1987); N. Nucker *et al.*, *ibid.* **37**, 5158 (1988).

[22]N. Nucker *et al.*, Z. Phys. B **67**, 9 (1987); A. J. Arko *et al.*, *ibid.* **40**, 2268 (1989).

[23]J. C. Fuggle, F. U. Hillebrecht, Z. Zolnierek, R. Lasser, Ch. Freiburg, O. Gunnarsson, and K. Schonhammer, Phys. Rev. B **27**, 7330 (1983).

[24]A. Fujimori, F. Minami, and S. Sugano, Phys. Rev. B **29**, 5225 (1984); D. D. Sarma and S. G. Ovchinnikov, *ibid.* **42**, 6817 (1990).

[25]J. Park, S. Ryu, M. Han, and S. J. Oh, Phys. Rev. B **37**, 10 867 (1988).

[26]H. Eskes and G. A. Sawatzky, Phys. Rev. B **43**, 119 (1991).